Defect dipole relaxation in polycrystalline dolomite [$CaMg(CO_3)_2$]

A. N. Papathanassiou and J. Grammatikakis
University of Athens, Department of Physics, Section of Solid State Physics, Panepistimiopolis, GR 15784 Zografos, Greece
(Received 5 October 1995)

The thermally stimulated depolarization current or ionic thermocurrent technique detects two low-temperature bands with maxima at 140 and 188 K, respectively. The choice of proper polarizing conditions, to inhibit the formation of space-charge polarization, permits the accurate study of the low-temperature mechanisms. The extensive dielectric characterization shows that the relaxation mechanisms are related to homogeneous polarization processes and most likely originate from dipolar centers. The thermal treatments indicate that the centers are probably defect dipole agglomerates. The energy parameters for dielectric relaxation are also evaluated. [S0163-1829(96)07123-8]

I. INTRODUCTION

Calcite ($CaCO_3$), magnesite ($MgCO_3$), and dolomite [$CaMg(CO_3)_2$ or $CaCO_3$:$MgCO_3$] belong to the so-called ''calcite family'' and crystallize in the rhombohedral crystal structure.[1,2] Dielectric studies on the calcite family will provide valuable information on the ionic relaxation of the mixed crystal dolomite [$CaMg(CO_3)_2$] in relation to the dielectric relaxation of the end members ($CaCO_3$ and $MgCO_3$). We notice that, to the best of our knowledge, little experimental work has been reported to date about the relaxation of mixed crystals.[3–6] From the calcite family, the only dielectric studies concern the calcite and limestone (polycrystalline rock-calcite).[7–9] Dolomite and magnesite have been studied very recently[10] and our results are in press.[11]

The present paper not only contributes to the pure research of ionic relaxation in the alkaline earth carbonate salts but can also assist in the improvement of the industrial and technological usage of these widespread salts.[12] Additionally, profit can be gained in the electrical geophysical processes, since the carbonate salts are important constituents of the Earth's crust.

II. THEORY

The dielectric relaxation of an insulator is due to the rotation of dipoles and to the motion of free charge barriers under certain boundary conditions.[13] The migration of the free charges, which themselves contribute to the dc conductivity, can be prohibited (i) from the internal obstacles (i.e., interfaces between two phases of different conductivities, grain boundaries, dislocations) leading to the interfacial (Maxwell-Wagner) polarization and (ii) from the non-Ohmic interface between the specimen surface and the electrodes, leading to the formation of space-charge polarization. Each of the relaxation phenomena, following the removal of an external polarizing field, is described by a relaxation time τ, which is temperature and pressure dependent. The relaxation time is related to the temperature via the Arrhenius equation

$$\tau(T)=\tau_0\exp(E/kT), \tag{1}$$

where E is the activation energy, τ_0 is the preexponential factor, and k is Boltzmann's constant.

In the thermally stimulated depolarization current (TSDC) method we can monitor the behavior of a previously polarized dielectric by varying the temperature. The basic steps are the following:[14] At a certain temperature T_p we polarize the sample for a period of time $t_p \gg \tau(T_p)$. Then keeping the external polarizing field on, we cool to liquid-nitrogen temperature (LNT) where the relaxation time is practically infinite. Therefore, upon switching off the field, the dielectric remains polarized. Subsequently, we detect with an electrometer the depolarization current as the temperature augments at a constant heating rate b. At the temperature range where the thermal energy competes with the energy E needed for the reorientation of the polarized dipoles, we get a transient electric signal called thermogram. For different types of dipoles, or for the dispersion of the frozen space-charge polarization, we get additional peaks.

In the simple case of noninteracting dipoles, the transient depolarization current density is

$$I(T)=\frac{S\Pi_0}{\tau_0}\exp\left[-\frac{E}{kT}-\frac{1}{b\tau_0}\int_{T_0}^{T}\exp\left(-\frac{E}{kT}\right)dT\right], \tag{2}$$

where Π_0 is the initial polarization of the dielectric, S is the sample's surface area, which is in contact to the electrode, and T_0 coincides with the LNT. The activation energy E is identical to the migration enthalpy h^m.

The relaxation time τ is given by the following relation (area method):

$$\tau(T)=\frac{1}{bI(T)}\int_{T}^{T_f}I(T)dT, \tag{3}$$

where T_f is the final temperature of the peak where the current becomes null. For the initial part of the curve, Eq. (2) reduces to

$$I(T)\cong\frac{S\Pi_0}{\tau_0}\exp\left(-\frac{E}{kT}\right). \tag{4}$$

For a linear heating rate b, the temperature $T_{\max}$ where the current maximizes is given through the equation:

$$\frac{T_{\max}}{\tau(T_{\max})} = \frac{Eb}{kT_{\max}}. \quad (5)$$

Equations (1) and (3) can lead to the evaluation of the activation energy E and to the value of the factor τ_0.

III. EXPERIMENTAL DETAILS

Our cryostat operates from LNT up to 400 K. A vacuum better than 10^{-6} mbars was created by an Alcatel molecular vacuum pump. The crystals were placed between the platinum electrodes and were polarized by using a Keithley 246 dc power supply. The temperature was measured by means of a gold-chromel thermocouple fed into the upper electrode, which was connected to an Air-Products temperature controller. The temperature rise was monitored by the controller and the desired (constant) heating rate was attained throughout each TSDC scan. The depolarization current was measured with a Cary 401 electrometer. Current intensities of the order of 10^{-16} A could be detected. The output signals from the controller and the electrometer were digitized via a Keithley DAS 8 PGA card installed into a computer. The data were afterwards analyzed with the appropriate software we have developed.

Details about the samples' origin and composition are given in the preceding paper.[15]

IV. RESULTS AND DISCUSSION

A. The way to perform reliable dielectric characterization

The common practice to obtain an ionic thermocurrent thermogram is to polarize the sample at room temperature (RT), where the dipole entities are mobile enough to orient. The situation becomes complicated when the dipolar mechanisms coexist with space-charge ones. The formation of the space-charge results in the creation of an internal electric field that opposes the external polarizing field. Subsequently, the total field that the dipoles feel during the polarization stage is reduced, probably to a null value in relation to the external field. Therefore, the polarization state of the dipole population can be altered drastically.[16] Additionally, as has already been reported, the nonuniform free charge distribution can lead to a polarization process of the dipoles during the heating of the sample and the simultaneous recording of the thermogram.[17]

In Fig. 1 we present the thermogram of polycrystalline dolomite obtained in the usual manner (T_p at RT). A strong complex mechanism, thereafter called HT, maximizes close to RT. Our recent extensive TSDC studies[10] prove that the HT band is related to the space-charge polarization. So, it would be risky to conclude that the HT peaks show the unique relaxation mechanism in dolomite, recalling that the space-charge formation might inhibit the dipole orientation.

The polarization state can be controlled drastically by the appropriate selection of the polarization time t_p and the polarization temperature T_p. If the polarization time t_p is too short and comparable to the time needed to cool the sample to LNT (a few seconds), there exists too large an uncertainty in the knowledge of the actual polarization time. So, t_p cannot easily be selected as the experimental parameter that will accurately control the polarization state attained. Instead, we keep t_p the same and choose T_p as the variable parameter so as to obtain high accuracy. In Fig. 2 we present the thermograms recorded by gradually decreasing the polarization temperature T_p. We observe that the degree of polarization of the HT band becomes smaller and, at the same time, the low-temperature (LT) spectra are exhibited. By polarizing at $T_p = 200$ K, the original uniform distribution of the space charge is not altered (the HT peak is not recorded at all), and we may get highly reproducible curves of the LT spectra. In the present paper, our interest will hereafter be focused in the LT spectra.

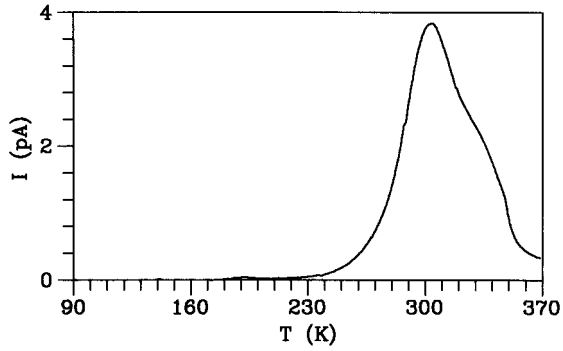

FIG. 1. TSDC thermogram of polycrystalline dolomite obtained in the usual manner, i.e., by polarizing at RT. The polarization conditions were $T_p = 292$ K, $t_p = 5$ min, $E_p = 7.09$ kV/cm. The heating rate was $b = 3.5$ K/min. The electrode material was platinum.

B. Variation of the polarization conditions, the electrode configuration, and the sample thickness

In Fig. 3 the LT spectra are depicted. They consist of two bands with maxima at 140 K (LT1 band) and 188 K (LT2 band). Since the mechanisms are also detected in monocrystal dolomite,[11] they are not determined by the material microstructure but rather by the ionic relaxation of the dolomite matrix.

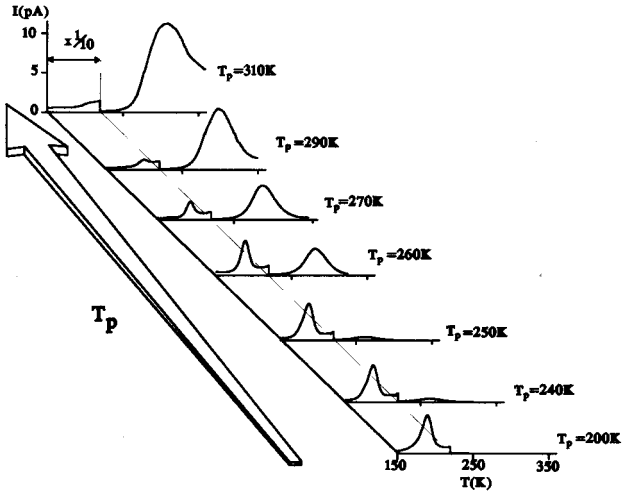

FIG. 2. Thermograms obtained by varying the polarization temperature T_p with the aim of preventing the space-charge polarization and obtaining reliable low-temperature dielectric characterization ($E_p = 21.43$ kV/cm, $t_p = 2$ min).

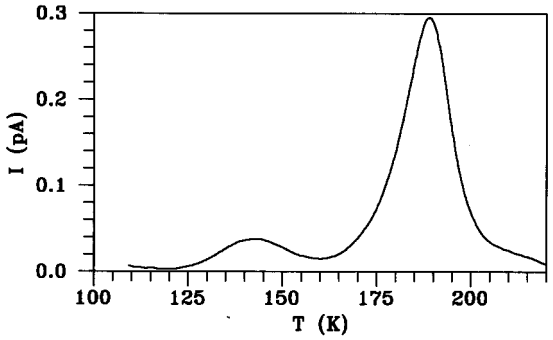

FIG. 3. The low-temperature (LT) spectra of an as-received sample of polycrystalline dolomite ($T_p=200$ K, $E_p=8.33$ kV/cm, $t_p=2$ min).

The vast majority of the experiments were performed by using platinum electrodes. We additionally used bronze electrodes, silver paste, graphite paint, and insulating (Teflon) electrodes (metal-insulator-sample-insulator-metal *MISIM* configuration).[14] In this way we could change the blocking degree of the electrodes. For each kind of electrode material we performed successive measurements under exactly the same polarization conditions ($T_p=200$ K, $E_p=6.94$ kV/cm, $t_p=2$ min) that lead to reproducible, electrode independent thermograms. The same set of experiments was performed by polarizing at $T_p=160$ K, so as to polarize only the LT1 mechanism and yielded the same conclusions. The high reproducibility and the invariance upon the nature of the electrodes strongly indicate the dipolar feature and the fact that the LT1 and LT2 mechanisms are related to the homogeneous polarization of the sample.

By polarizing at $T_p=200$ K ($E_p=6.76$ kV/cm) and choosing different values of the polarization time t_p (1, 2, 3, 4, 6, and 9 min), we observed that the saturation was attained at about 1 min. By selecting $T_p=160$ K, $E_p=7.14$ kV/cm and varying the t_p values (15 sec, 1, 2, and 3 min), we found the saturation polarization again at about 1 min. This behavior for the attainment of saturation is characteristic of dipoles.

While keeping E_p and t_p constant, we changed T_p. For T_p larger than 140 and 188 K, the maxima of LT1 and LT2, respectively, remained the same. When $T_p<140$ K the temperature $T_{\max}$ (at which LT1 maximizes) and the peak amplitude $I_{\max}$ decrease upon T_p (Fig. 4). The phenomenon can

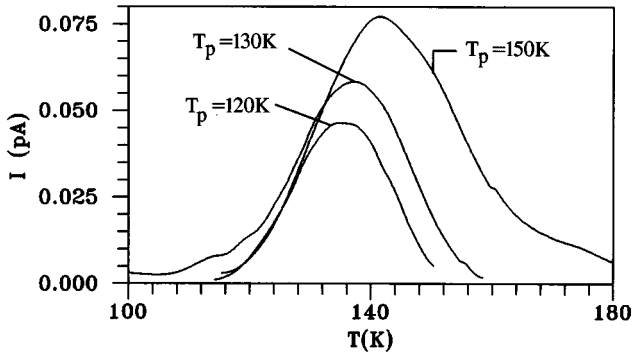

FIG. 4. Dependence of the LT1 band upon the polarization temperature T_p ($E_p=6.76$ kV/cm, $t_p=2$ min).

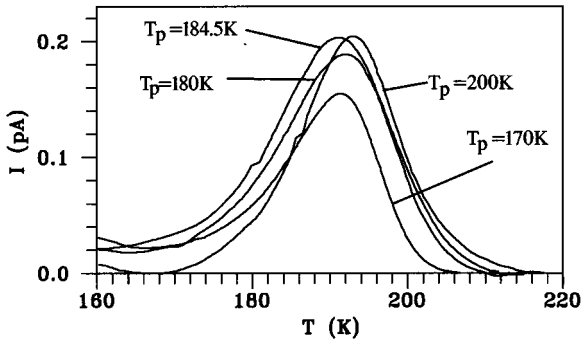

FIG. 5. Dependence of the LT2 band upon the polarization temperature T_p ($E_p=6.76$ kV/cm, $t_p=2$ min). By polarizing at $T_p=160$ K, LT1 is not polarized at all.

be interpreted via the relaxation time distribution model and can be viewed as the polarization of the faster components upon T_p decrease. On the contrary, the LT2 peak location remains unaltered (Fig. 5) by shifting T_p to lower temperatures, indicating a unique relaxation time response.

In Fig. 6 we display the dependence of the polarization state upon the external electric field intensity E_p. The linearity is typical of dipole relaxation, although this result cannot be considered as a proof of the dipolar character.

For two different polarization temperatures ($T_p=160$ and 200 K) and keeping the polarization conditions constant ($E_p=9.09$ kV/cm, $t_p=2$ min), we examined the dependence of the signal upon the sample thickness. The initial thickness was 1.65 mm and the final one 0.90 mm. As can be seen in Fig. 7, the spectrum remains unaffected, indicating that the relaxation mechanisms of both LT1 and LT2 are related to the homogeneous polarization of the sample.[14,18]

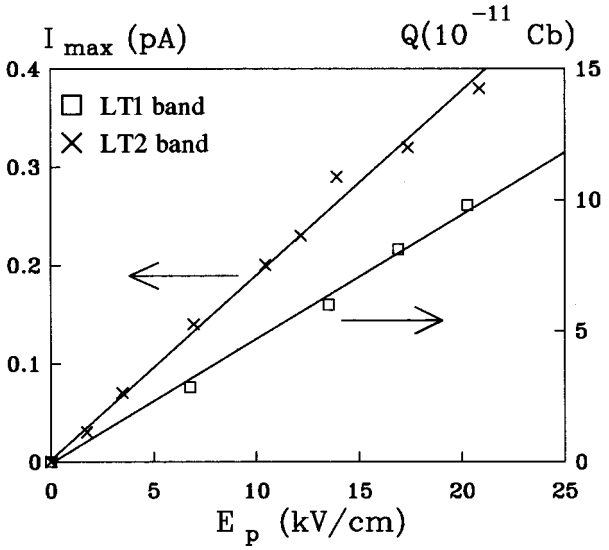

FIG. 6. Dependence of the signal upon the electric field intensity E_p. The data for the LT1 band were obtained by polarizing at $T_p=160$ K, while for the LT2 band by polarizing at $T_p=200$ K. The polarization state of the LT1 band is described by the total charge Q released. Due to the fact that LT2 overlaps with LT1, the polarization state of LT2 is more reliably represented by the peak amplitude $I_{\max}$.

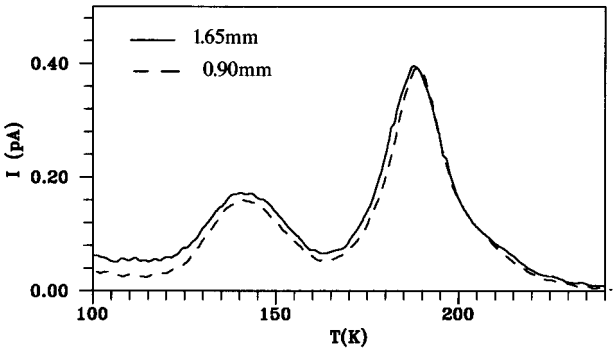

FIG. 7. Thermograms for two different thickness values of the same sample ($T_p=200$ K, $E_p=9.09$ kV/cm, $t_p=2$ min).

C. Resolution of the relaxation components and evaluation of the energy parameters

The partial heating technique was applied in ionic crystals by us[19] and consists of the following steps: After polarization at 200 K and cooling down to LNT, we heat up the sample until we get the initial rise of the thermocurrent and immediately cool down to LNT. If T_c denotes the cooling temperature, we repeat the heating procedure by a gradual increase of T_c, until we discharge the sample completely. The set of initial rise curves provides, through Eq. (4), the activation energy E distribution versus the temperature. The advantage of the technique is that the initial rise, as stated in the theory, is described via Eq. (4) for any kind of mechanism (dipoles or space charge). In Fig. 8 we see that the activation energy values distribute from 0.24 to 0.40 eV for the LT1 band and scatter from 0.50 to 0.61 eV for LT2. The wide energy distribution of LT1 is to be expected since the aforementioned variation of $T_{\max}$ upon T_p, for $T_p<140$ K, indicates the distribution of the relaxation time. Due to the fact that the LT2 band does not show any distribution in τ, we must attribute the scatter to a weak peak, satellite to the LT2 dispersion. This aspect is indeed justified in the following paragraph.

In Fig. 9 we have separated the dominant mechanism (labeled LT2a) by polarizing at $T_p=166$ K. Due to the overlap of the LT2 band with the LT1, we partially discharged the material during the heating stage up to 170 K, cooled once more to the LNT and, in the second run, we got the whole LT2a component. In Fig. 10 we have plotted the $\ln\tau$ values for LT2a, according to Eq. (3), vs T^{-1}. The excellent linearity certifies the good isolation and verifies the aspect that the relaxation is due to single value τ rotating dipoles.

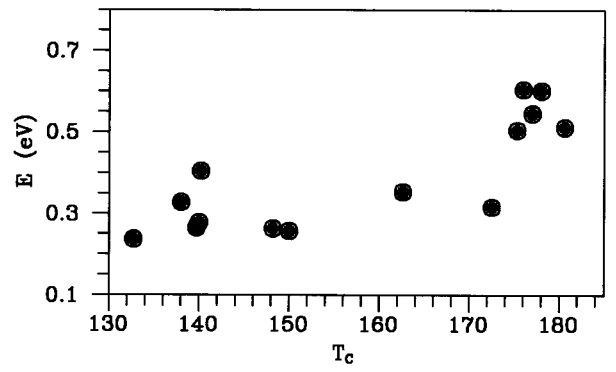

FIG. 8. Temperature dependence of the activation energy E evaluated from a set of initial rise curves obtained by employing the partial heating scheme. T_c denotes the end temperature of the initial rise curve, where the sample is cooled down to LNT.

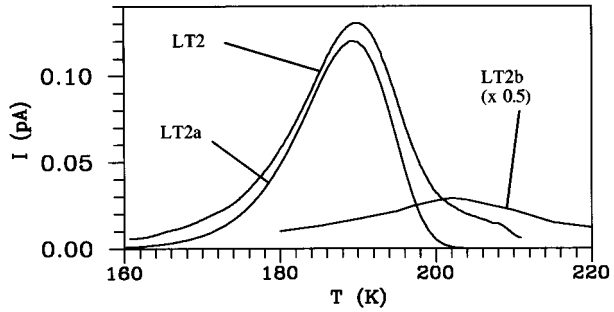

FIG. 9. The LT2 band was obtained under the polarization conditions: $T_p=200$ K, $E_p=6.76$ kV/cm, $t_p=2$ min. Its dominant component LT2a was obtained by choosing $T_p=166$ K, $E_p=6.76$ kV/cm, $t_p=2$ min and partially discharging up to 170 K. The satellite weak peak (LT2b) was obtained by initially choosing $T_p=200$ K, $E_p=6.76$ kV/cm, $t_p=2$ min and partially discharging up to 200 K.

The energy parameters obtained from the Arrhenius plot are depicted in Table I. We notice that the maximum of LT2a coincides with that of LT2 and that the amplitude of LT2a strongly dominates that of LT2. Therefore, we may identify the features of LT2, reported above, with those of its very dominant component LT2a. By polarizing at $T_p=200$ K and after partially discharging up to 200 K, we obtained a weak satellite peak, labeled LT2b. From the initial rise analysis [Eq. (4)] and the maximum condition [Eq. (5)] we evaluated the energy parameters of LT2b that are displayed in Table I.

D. The effect of thermal treatment

The dolomite samples were thermally treated in two different ways: In the first one, the anneal was performed at 400 °C for 30 min (Fig. 11) and, in the latter, inside the cryostate (in vacuum) at 150 °C for 2 h. In both cases, the thermal anneal was followed by rapid quench to the RT. The electrode material was platinum, but graphite paint was additionally used in some specimens. The sample's weight did

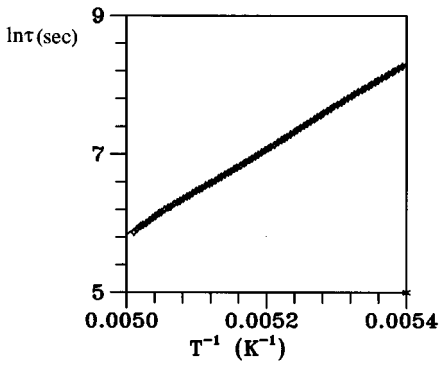

FIG. 10. The Arrhenius plot of the component LT2a. The energy parameters evaluated from the diagram are depicted in Table I.

TABLE I. Energy parameters of the low-temperature mechanisms. Techniques of parameter evaluation: *: partial heating; **: peak cleaning (area and computer fitting); and ***: partial discharge (initial rise method).

	E (eV)	τ_0 (sec)
LT1 (*)	0.24–0.40	
LT2 (*)	0.50–0.61	
LT2a (**)	0.53	1.22×10^{-11}
LT2b (***)	0.39	2.41×10^{-8}

not change after the anneal. The thermograms recorded after the thermal perturbation indicated the following.

(a) The amplitude of LT2 is reduced to approximately 60% of the original spectrum, while $T_{\max}$ remains unaffected after the thermal treatment.

(b) The shape of the LT2 band is the same as a simple single peak, like LT2a. The Arrhenius plot is a straight line that leads to the energy parameters: $E=0.55$ eV and $\tau_0=6.861\times10^{-13}$ sec. In view of the fact that the maximum temperature $T_{\max}$ and, in comparison to the values reported in Table I, the energy parameters are practically the same as those of the virgin samples, we can state that the LT2a band survives the thermal treatment, probably by partial aggregation of the dipoles to some larger aggregates with null dipolar moment (considering the fact that no additional peak appears following the thermal treatment).

(c) LT1 is shifted to lower temperatures (the maximum is located to $T_{\max}=130$ K) without variation of the charge released.

(d) Two months after the thermal treatment, the spectrum consists of a broad LT1 band maximizing around 155 K, whereas the total charge released remains almost the same in comparison to the virgin spectrum band. The LT2 band remains the same as that detected immediately after the quench.

Observations (a) and (b) are typical of defect dipole centers.[19] Due to the fact that the position and the energy parameters of LT2 practically remain unaltered, we conclude that a considerable number (approximately 60%) of the dipoles keep their structural configuration, while the others are either decomposed to simpler aggregates or else form some larger agglomerates with zero dipole moment. If any conversion of the LT2a dipoles to LT1 ones happened, then the LT1 amplitude should increase, but this is not justified by observation (c). Observations (c) and (d) indicate that the thermal treatment affects the distribution of the relaxation time, leading to different maxima $T_{\max}$ of LT1.

E. On the origin of the dipole bands

We conclude that the sensitivity of the low-temperature mechanisms to the thermal treatment directs us to the aspect of the defect dipole rotation. The configuration of these centers cannot be understood via dielectric measurements, unless we exploit the dielectric properties of the calcite family and profit from additional spectroscopic data. For the calcite family [calcite ($CaCO_3$), magnesite ($MgCO_3$), and dolomite $CaMg(CO_3)_2$] there has already been reported a band corresponding to LT2 as the unique dipole relaxation band in calcite. Our work on magnesite shows that the LT1 mechanism is the only dipolar relaxation mechanism appearing in the thermograms. As both LT1 and LT2 appear in the thermograms of dolomite, we can conclude that the LT1 mechanism originates from the defect structure of the magnesium sublattice, whereas LT2 is related to the defect structure of the calcium sublattice.[11]

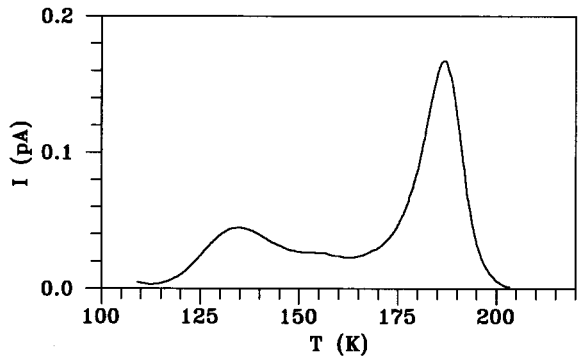

FIG. 11. Thermogram of a sample annealed at 400 °C for 30 min and subsequently quenched to RT. The polarization conditions were $T_p=200$ K, $E_p=8.33$ kV/cm, $t_p=2$ min.

It was verified spectroscopically that Mn^{2+} impurity is favored in dolomite,[20,21] therefore it might contribute to the defect structure in the magnesium sublattice,[22] stimulating the LT1 mechanism. From another viewpoint, the temperature region where LT1 appears is typical for a wide variety of materials that contain water in their structure.[23] Our analyses showed that our materials contain a small amount of water (free water or hydroxyl) incorporated into the matrix, and having in mind that hydroxyl incorporation is favored in the magnesium sublattice,[24] we may be justified in attributing the LT1 band to dipoles where hydroxyl is the basic component.

The LT2 mechanism can be related to the defect dipoles, with Sr^{2+} (Ref. 25) or Al^{3+} as the most probable candidates.[11]

V. CONCLUSION

The formation of the space charge during the polarization stage in a TSDC experiment in polycrystalline dolomite strongly affects the orientation of dipoles and strongly alters the low-temperature spectra. The proper dielectric characterization of the dipolar mechanisms was attained by appropriate selection of the polarization temperature T_p, which prevents the space-charge polarization. Two bands, typical for the dolomite material, labeled LT1 and LT2, show maxima at 140 and 188 K, respectively. By changing the electrode material, the polarization conditions, the sample thickness and by employing different thermal treatments, we proved that the bands originate from the relaxation of defect dipoles. LT1 is related to the defect structure developed in the magnesium sublattice, while LT2 is related to that developed in the calcium sublattice. Mn^{2+} or hydroxyl complexes are possible candidates for the appearance of LT1, and LT2 might be related to Sr^{2+} or Al^{3+} defect dipoles.

[1] M.H. Battey, *Mineralogy for Students* (Longman, London, 1981).
[2] W.A. Deer, R.A. Howie, and J. Zussman, *An Introduction to the Rock Forming Minerals* (Longman, Essex, 1966).
[3] R. Robert, R. Barboza, G.F.L. Ferreira, and M. Ferreira de Souza, Phys. Status Solidi B **59**, 335 (1973).
[4] S.C. Zílio and M. de Souza, Phys. Status Solidi B **80**, 597 (1977).
[5] T. Ohgaku and N. Takeuchi, Phys. Status Solidi A **42**, K83 (1977).
[6] M.V.S. Sarma and S.V. Suryanarayana, J. Mater. Sci. Mater. Electron. **1**, 182 (1990).
[7] N.G. Bogris, J. Grammatikakis, and A.N. Papathanassiou, in *Proceedings of the XII International Conference on Defects in Insulating Materials ICDIM92, Germany, 1992*, edited by O. Kanert and J.-M. Spaeth (World Scientific, Singapore, 1993), p. 804.
[8] N. Bogris, Ph.D. Dissertation, University of Athens, 1993 (unpublished).
[9] J.F. de Lima, E.M. Yoshimura, and E. Okuno (unpublished).
[10] A.N. Papathanassiou, Ph.D. Dissertation, University of Athens, 1995.
[11] A.N. Papathanassiou, J. Grammatikakis, V. Katsika, and A.B. Vassilikou-Dova, Radiat. Eff. Def. Solids **134**, 247 (1995).
[12] A. Baysar and J.L. Kuester, IEEE Trans. Microwave Theory Tech. **40**, 2108 (1992).
[13] A.K. Jonscher, *Dielectric Relaxation in Solids* (Chelsea Dielectrics Press, London, 1983).
[14] J. Vanderschueren and J. Gasiot, in *Thermally Stimulated Relaxation in Solids*, edited by P. Braunlich (Springer-Verlag, Berlin, 1979).
[15] A.N. Papathanassiou and J. Grammatikakis, preceding paper, Phys. Rev. B **53**, 16 247 (1996).
[16] Da Yu Wang and A.S. Nowick, Phys. Status Solidi A **73**, 165 (1982).
[17] N. Suarez, M. Puma, E. Laredo, and D. Figueroa, Cryst. Latt. Def. Amorph. Mat. **15**, 283 (1987).
[18] J. van Turnhout, *Thermally Stimulated Discharge of Polymer Electrets* (Elsevier, Amsterdam, 1975).
[19] A.N. Papathanassiou, J. Grammatikakis, and N. Bogris, Phys. Rev. B **48**, 17 715 (1993).
[20] G. Calas, in *Reviews in Mineralogy Vol. 18: Spectroscopic Methods in Mineralogy and Geology*, edited by F.C. Hawthorne (Mineralogical Society of America, Washington, D.C., 1988).
[21] A.B. Vassilikou-Dova and G. Lehmann, Fortschr. Miner. **65**, 173 (1987).
[22] F. Prissok and G. Lehmann, Phys. Chem. Minerals **13**, 331 (1986).
[23] P. Pissis, D. Anagnostopoulou-Consta, L. Apekis, D. Daoukaki-Diamanti, and C. Christodoulides, J. Non. Cryst. Solids **1174-1181**, 131 (1991).
[24] F.T. Mackenzie, W.D. Bischoff, F.C. Bishop, M. Loijens, J. Schoonmaker, and R. Wollast, in *Reviews in Mineralogy, Vol. 11, Carbonates: Mineralogy and Chemistry*, edited by R.J. Reeder (Mineralogical Society of America, Washington, D.C., 1983).
[25] J. Veizer, in *Reviews in Mineralogy, Vol. 11, Carbonates: Mineralogy and Chemistry*, edited by R.J. Reeder (Mineralogical Society of America, Washington, D.C., 1983).